MRR-PRO

Description of products

Valid for MRR-PRO-Firmware VS≥01

METEK
Meteorologische Messtechnik GmbH

Fritz-Strassmann-Strasse 4
D-25337 Elmshorn
Germany

Fon +49 4121 4359-0
Fax +49 4121 4359-20
e-mail info@metek.de
internet http://www.metek.de

Previous update: 08 October 2020
Last update : 04 August 2021

Table of content

T

1 Calculation of Products

Nomenclature:

For most variables and parameters in the following aliases are given in single quotes. These are the names of variables used in the NetCdf-files. The names in ASCII-files are different. See manual for details.

1.1 Raw spectra $s_r(i,n)$, 'spectrum_raw', incoherent averaging

The raw spectral power is stored in engineering units. It is linearly related to the power at the receiver input in each spectral line. The actual numeric values are determined by the (frequency dependent) receiver gain, the ADC resolution and subsequent spectral processing. The transformation into physically meaningful units is done in the course of reflectivity spectra calculation (see chapter 1.2).

MRR-PRO issues $\boldsymbol{s_r} = 10\log_{10} s_r$ (decibel).

Due to the arbitrary phases of superposed signal contributions from randomly distributed particles in the scattering volume the resulting spectral power is randomly distributed according to an exponential distribution with a standard deviation that is incidentally equal to the expectation value of the power. It is therefore desirable to reduce the stochastic component by averaging ensembles of power spectra. Averaging over I power spectra reduces the standard deviation by $1/\sqrt{I}$ in the limit of $I \gg 1$, if the time step Δt of subsequent spectra is longer than the signal coherence time τ_c (Averaging with $\Delta t > \tau_c$ is referred to as incoherent averaging). The rate at which power spectra are generated by the FMCW- algorithm depends on the number of spectral lines m, the number of range gates N and the sampling rate f_s. If the width of the dominant peak of observed spectra is larger than the spectral resolution, one may assume that the condition $\Delta t > \tau_c$ is fulfilled.

Example: The sampling rate of MRR-PRO is fixed at 500 kHz. A typical setting of $m = 64$, $N = 128$ and averaging time $T_I = 10$ s leads to $I = 305$, if the velocity distribution width is larger than 0.19 m/s. This is always the case for rain echoes. (See chapter 2.2 for general relations.) In this example, the standard deviation of the spectral power relative to the expectation value is reduced to 5.7% or 0.24 dB.

1.2 Reflectivity spectra $\eta_a(i,n)$, 'spectrum_reflectivity', calibration, attenuation

Before converting raw spectra into calibrated reflectivity spectra the noise background is estimated and subtracted from the raw spectral power using a method similar to Hildebrand and Sekhon (1974). (See document "20210729-MRR-PRO-Noise.pdf" for details.) The uncertainty of estimation leads to some false alarm rate which can be estimated based on the sample size. The detection limit is set to a level corresponding to an estimated false alarm rate of 10^{-4}. The remaining spectral signal power after nose subtraction $s(i,n)$ is converted into attenuated reflectivity $\eta_a(i,n)$ for spectral line number $i = 1 \ldots m$ and for range gate number $n = 1 \ldots N$ by invoking the radar equation. For beam filling targets and ignoring the attenuation due to extinction processes this equation reads

$$\eta_a(i,n) = s(i,n)\frac{C}{T(n)}n^2\delta r \qquad \text{Eq. 1-1}$$

with $\delta r =$ range resolution (a configurable radar operation parameter), $C =$ radar 'calibration constant', and $T(n) =$ 'transfer function'. The radar calibration constant includes the transmit power, the effective antenna area, and internal signal losses. The transfer function describes the frequency dependent gain of the receiver. In case of FMCW radar, this translates into a receiver gain depending on the range gate number n.

MRR-PRO issues $\eta = 10 \log_{10} \eta$ (decibel).

1.3 Attenuated drop size distributions $N_a(D, n)$, 'N'

For the derivation of drop size distributions, we substitute the independent variable i by D. This substitution occurs in two steps.

First step:

The spectral line number i is substituted by the velocity v using

$$\eta_a(v, n) = \eta_a(i, n) \frac{\partial i}{\partial v} \qquad \text{Eq. 1-2}$$

From

$$v = i * \delta v \qquad \text{Eq. 1-3}$$

follows

$$\frac{\partial i}{\partial v} = \frac{1}{\delta v} \qquad \text{Eq. 1-4}$$

with $\delta v =$ velocity resolution. δv depends the chosen radar operation parameters according to Eq. 2-16.

Insertion of Eq. 1-4 into Eq. 1-2 yields

$$\eta_a(v, n) = \frac{\eta_a(i, n)}{\delta v} \qquad \text{Eq. 1-5}$$

Second, the velocity is substituted by the drop diameter D using

$$\eta_a(D, n) = \eta_a(v, n) \frac{\partial v}{\partial D} \qquad \text{Eq. 1-6}$$

For this substitution, it is assumed that v represents the terminal fall velocity of rain drops of diameter D.

The relation between v and D has been put into an analytical form by Atlas (1973) in the diameter range $D_{\min} = 0.109$ mm to $D_{\max} = 6$ mm, and is based on measurements by Gunn and Kintzer (1949). We use a form in which a height dependent correction for air density $\delta_\rho(h)$ is included for the fall velocity:

$$v(D,h) = \{9.65 - 10.3 \cdot \exp(-600 \cdot D)\}\delta_\rho(h) \quad \text{Eq. 1-7}$$

with $v(D,h)$ in ms^{-1} and D in m.

Foote and duToit (1969) suggested the approximative correction factor

$$\delta_\rho(n) = 1 + 3.68 \cdot 10^{-5} n\boldsymbol{\delta r} + 1.71 \cdot 10^{-9}(n\boldsymbol{\delta r})^2 \quad \text{Eq. 1-8}$$

This approximation implies US Standard Atmosphere conditions. The derivative of Eq. 1-7 with respect to D is

$$\frac{\partial v}{dD} = 6.18 \cdot \exp(-600 \cdot D)\delta_\rho(n) \quad \text{Eq. 1-9}$$

Insertion into Eq. 1-6 yields

$$\eta_a(D,n) = 6.18 \cdot \eta_a(v,n)\exp(-600 \cdot D)\delta_\rho(n) \quad \text{Eq. 1-10}$$

We assume that the reflectivity $\eta_a(D,n)$ is caused by rain drops with the backscatter cross section $\sigma(D)$, which can be calculated by Mie-theory (Mie, 1908). Then the attenuated spectral number density follows from

$$N_a(D,n) = \frac{\eta_a(D,n)}{\sigma(D)} \quad \text{Eq. 1-11}$$

1.4 Path integrated attenuation PIA, 'PIA'

Electromagnetic waves propagating through rain are attenuated due to absorption and scattering at rain drops. This occurs both on the path from the radar to the scattering volume and on the return path. The ratio between the received power without and with attenuation is called path integrated attenuation PIA. It could be calculated immediately, if the range resolved drop size distribution on the propagation path would be known. Unfortunately, Eq. 1-11 specifies only the attenuated drop size distribution.

If we assume that PIA can be neglected in the first range gate, PIA of more distant range gates can be estimated based on $N_a(D,n)$ as shown in the flow chart below.

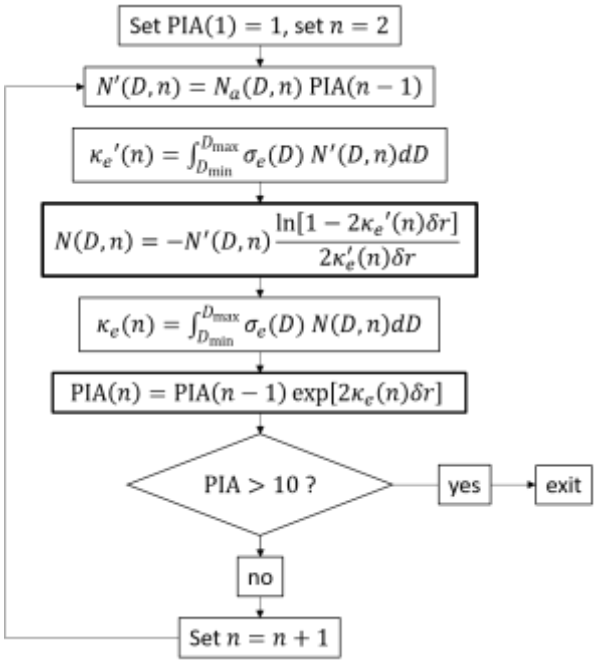

κ_e is the specific rain attenuation and σ_e is the single particle extinction coefficient, which is calculated with Mie-theory. The thick framed boxes contain the results, namely the path integrated attenuation and the attenuation-corrected drop size distribution. Since the algorithm becomes very unstable at larger values of PIA, the calculation stops, if PIA exceeds 10.

A more detailed discussion of attenuation correction algorithms can be found in Peters et al. (2010).

MRR-PRO issues $\mathbf{PIA} = 10 \log_{10} \mathrm{PIA}$.

The following products are attenuated and corrected by multiplication with PIA:

Drop Size Distribution
Radar Reflectivity Factor
Equivalent Radar Reflectivity Factor
Liquid Water Content
Rain Rate

All profiles of attenuation corrected products terminate at the height, where PIA exceeds 10.

1.5 Drop size distribution $N(D)$, 'N'

The drop size distribution $N(D)$ is related to the attenuated drop size distribution $N_a(D)$ (described in chapter 1.3) by

$$N(D) = N_a(D)\mathrm{PIA} \qquad \text{Eq. 1-12}$$

$N(D)$ is the number of drops in the scattering volume, divided by the size of the scattering volume, differentiated with respect to D at the diameter D. The unit is m^{-4}.

1.6 Radar reflectivity factor Z, 'Z'

The radar reflectivity factor is defined and calculated by

$$Z = 10^{18} \int_{D_{\min}}^{D_{\max}} N(D)\, D^6 dD \qquad \text{Eq. 1-13}$$

By convention the scattering volume is given in m^3 and the drop diameter in mm. Therefore, the unit of Z is $\mathrm{m}^{-3}\mathrm{mm}^6$.

MRR-PRO issues $\boldsymbol{Z} = 10 \log_{10} Z$.

1.7 Attenuated radar reflectivity factor Z_a, 'Za'

As mentioned in chapter 1.4, attenuation corrected results are suppressed, if PIA exceeds 10. For some applications, the knowledge of the attenuated version of some products at larger heights is nevertheless useful. A typical scenario is snowfall, as in this case the attenuation is overestimated and the actual attenuation may be even negligible.

Therefore, also the attenuated reflectivity factor

$$Z_a = 10^{18} \int_{D_{\min}}^{D_{\max}} N_a(D)\, D^6 dD = Z/\mathrm{PIA} \qquad \text{Eq. 1-14}$$

is calculated.

MRR-PRO issues $\boldsymbol{Z}_a = 10 \log_{10} Z_a$.

1.8 Equivalent radar reflectivity factor Z_e, 'Ze'

The reflectivity η is obtained by integration over the reflectivity spectrum

$$\eta = \int_{v_{\min}}^{v_{\max}} \eta(v) dv \quad \text{or} \quad \eta = \int_{D_{\min}}^{D_{\max}} \eta(D) dD \qquad \text{Eq. 1-15}$$

In the right-side form of Eq. 1-15 $\eta(D)$ can be replaced by $\sigma(D)N(D)$

$$\eta = \int_{D_{\min}}^{D_{\max}} \sigma(D) N(D) dD \qquad \text{Eq. 1-16}$$

For drop sizes much smaller than the radar wave length (Rayleigh-approximation) the backscattering cross section can be expressed by

$$\sigma(D) \cong \frac{\pi^5}{\lambda^4} |K|^2 D^6 \qquad \text{Eq. 1-17}$$

where $K = (m^2 - 1)/(m^2 + 2)$ and $m = n - jn\kappa$ is the complex refractive index. By inserting $\sigma(D)$ of Eq. 1-17 into Eq. 1-16 we obtain

$$\eta = \frac{\pi^5}{\lambda^4}|K|^2 \int_{D_{\min}}^{D_{\max}} N(D)\, D^6 dD \qquad \text{Eq. 1-18}$$

or

$$\eta = 10^{-18}\frac{\pi^5}{\lambda^4}|K|^2 Z \qquad \text{Eq. 1-19}$$

Inverted

$$Z_{(e)} = 10^{18}\frac{\lambda^4}{\pi^5|K|^2}\eta \qquad \text{Eq. 1-20}$$

Eq. 1-20 is the common relation used by weather radars for deriving Z from the reflectivity. This relation takes for granted that the Rayleigh approximation is applicable for all drop sizes. If it is applied to the reflectivity measured at 24 GHz (MRR-PRO frequency), this condition is not necessarily met. Nevertheless, there are applications where this relation is useful also at non-Rayleigh frequencies. The result is then called equivalent radar reflectivity factor Z_e as reminder that Z_e may deviate from Z.

MRR-PRO issues $\boldsymbol{Z_e} = 10\log_{10} Z_e$.

1.9 Attenuated equivalent reflectivity factor Z_{ea}, 'Zea'

With similar arguments as in chapter 1.7, also an attenuated version of the equivalent reflectivity factor is issued.

$$Z_{ea} = 10^{18}\frac{\lambda^4}{\pi^5|K|^2}\eta_a = Z_e/\mathrm{PIA} \qquad \text{Eq. 1-21}$$

with

$$\eta_a = \int_{D_{\min}}^{D_{\max}} \eta_a(D) dD = \eta/\mathrm{PIA} \qquad \text{Eq. 1-22}$$

MRR-PRO issues $\boldsymbol{Z_{ea}} = 10\log_{10} Z_{ea}$.

1.10 Liquid water content LWC, 'LWC'

The liquid water content is the product of the total volume of all droplets with the density of water ρ_w, divided by the scattering volume. It is therefore proportional to the 3rd moment of the drop size distribution:

$$\mathrm{LWC} = \rho_w \frac{\pi}{6}\int_{D_{\min}}^{D_{\max}} N(D) D^3 dD \qquad \text{Eq. 1-23}$$

1.11 Rain rate RR, 'RR'

The differential rain rate $\mathrm{rr}(D)$is equal to the volume of the differential droplet number density multiplied with the corresponding terminal fall velocity $(\pi/6)N(D)v(D)$. From this product, the rain rate is obtained by integration over the drop size:

$$\mathrm{RR} = \frac{\pi}{6}\int_{D_{\min}}^{D_{\max}} N(D)D^3 v(D)dD \qquad \text{Eq. 1-24}$$

1.12 Characteristic fall velocity VEL, 'VEL'

Various definitions for the characteristic fall velocity are possible. Here, the first moment of the Doppler spectra is chosen, because this is the usual way of radar wind profilers to determine radial velocities

$$i_1 = \frac{\int_{i=1}^{i=\boldsymbol{m}} \eta_a(i) i di}{\int_{i=1}^{i=\boldsymbol{m}} \eta_a(i) di} \qquad \text{Eq. 1-25}$$

and

$$\mathrm{VEL} = \frac{\lambda}{2}\delta f i_1 \qquad \text{Eq. 1-26}$$

VELdoes not depend on the attenuation, because PIA cancels in the numerator and denominator of Eq. 1-25. Therefore, the profiles of VEL do not terminate at $\mathrm{PIA} > 10$.

1.13 Spectral width WIDTH, 'WIDTH'

The second moment of the spectra is calculated according to

$$i_2^2 = \frac{\int_{i=1}^{i=\boldsymbol{m}} \eta_a(i)(i-i_1)^2 di}{\int_{i=1}^{i=\boldsymbol{m}} \eta_a(i) di} \qquad \text{Eq. 1-27}$$

and

$$\mathrm{WIDTH} = \frac{\lambda}{2}\delta f i_2 \qquad \text{Eq. 1-28}$$

WIDTH does not depend on the attenuation, because PIA cancels in the numerator and denominator of Eq. 1-27. Therefore, the profiles of WIDTH do not terminate at $\mathrm{PIA} > 10$.

1.14 Signal to noise ratio SNR, 'SNR'

The signal power S is estimated by integrating the spectral signal power in the -10 dB-environment of the spectral peak.

$$S = \int_{i_{\mathrm{low}}}^{i_{\mathrm{high}}} s(i)di \qquad \text{Eq. 1-29}$$

The integration limits i_{low} and i_{high} are indicated in the figure below.

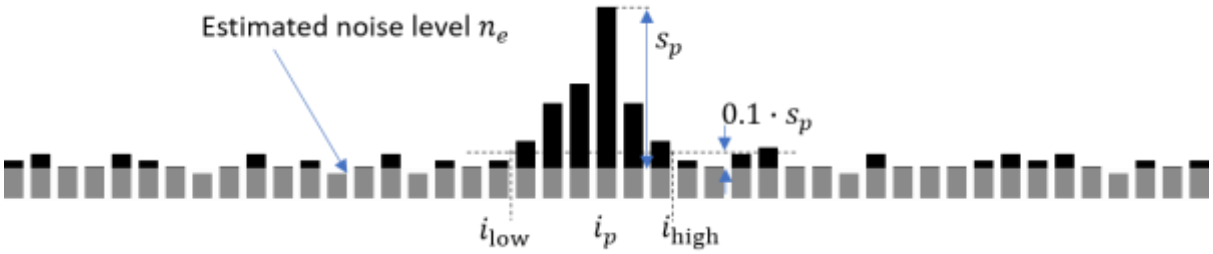

The spectral power below the estimated noise level is grey-shaded. The black area between i_{low} and i_{high} is the signal power S, and the grey-shaded area is the corresponding noise power

$$N_e = n_e \cdot \left(i_{\mathrm{high}} - i_{\mathrm{low}}\right) \qquad \text{Eq. 1-30}$$

The signal to noise ratio is

$$\mathrm{SNR} = \frac{S}{N_e} \qquad \text{Eq. 1-31}$$

MRR-PRO issues $\mathbf{SNR} = 10 \log_{10} \mathrm{SNR}$.

The profiles of **SNR** are issued unconditionally, i.e. they include heights with $\mathrm{PIA} > 10$ and even heights where the false alarm rate exceeds 10^{-4}

1.15 Melting layer ML, 'ML'

Profiles of reflectivity, velocity and spectral width are analyzed for detection of the melting layer. The reflectivity is enhanced in the upper part of the ML because snow crystals are covered by a wet skin with larger refractive index than ice. In the lower part the crystal aggregates collapse to water drops with reduced scattering cross section due to the reduced size. The fall velocity accelerates during the melting process, because the air drag of water droplets is smaller than that of mass-equivalent snow crystals. The spectra width increases because the fall velocity of water droplets show a broad distribution according to the size distribution. Snow flakes on the other hand fall with nearly uniform speed which is only weakly dependent on the mass. The probability of ML-detection is indicated at each range gate by a number between 0 (Certainly no ML) and 1 (Certainly ML). Multiple MLs can be detected.

2 MRR-PRO Operation Parameters

2.1 List of parameters

Explicitly configurable

$\boldsymbol{N}$: Number of range gates

$\boldsymbol{m}$: Number of lines in spectrum

$\boldsymbol{T_i}$: Time of incoherent averaging

$\boldsymbol{\delta r}$: Range resolution

Fixed

$\boldsymbol{f_s}$: Sampling rate $= 500$ kHz

$\boldsymbol{\lambda}$: Wavelength $= 1.238 \cdot 10^{-2}$ m

$\boldsymbol{c}$: Velocity of light (in air)$= 2.997 \cdot 10^{8}$ ms^{-1}

Dependent

B: Signal bandwidth

I: Number of incoherently averaged spectra

M: Number of sweeps for a single measurement

T_s: Sweep time

f_{ny}: Nyquist frequency range

v_{ny}: Nyquist velocity range

δf: Frequency resolution

δt: Time resolution of one spectrum (single measurement)

δv: Velocity resolution

H: Height range

2.2 Dependence between parameters

$$T_s = \frac{2\boldsymbol{N}}{\boldsymbol{f_s}} \quad \text{Eq. 2-1}$$

$$f_{ny} = \frac{1}{T_s} \quad \text{Eq. 2-2}$$

$$f_{ny} = \frac{\boldsymbol{f_s}}{2\boldsymbol{N}} \quad \text{Eq. 2-3}$$

$$v_{ny} = \frac{\boldsymbol{\lambda} f_{ny}}{2} \quad \text{Eq. 2-4}$$

$$v_{ny} = \frac{\boldsymbol{\lambda}}{2T_s} \quad \text{Eq. 2-5}$$

$$v_{ny} = \frac{\boldsymbol{\lambda f_s}}{4\boldsymbol{N}} \quad \text{Eq. 2-6}$$

$$M = \boldsymbol{m} \quad \text{Eq. 2-7}$$

$$\delta t = \boldsymbol{m} T_s \quad \text{Eq. 2-8}$$

$$\delta f = \frac{1}{\delta t} \quad \text{Eq. 2-9}$$

$$\delta f = \frac{1}{\boldsymbol{m} T_s} \quad \text{Eq. 2-10}$$

$$\delta f = \frac{f_{ny}}{\boldsymbol{m}} \quad \text{Eq. 2-11}$$

$$\delta f = \frac{\boldsymbol{f_s}}{2\boldsymbol{m}\boldsymbol{N}} \quad \text{Eq. 2-12}$$

$$\delta v = \frac{\boldsymbol{\lambda}\delta f}{2} \quad \text{Eq. 2-13}$$

$$\delta v = \frac{\boldsymbol{\lambda}}{2\delta t} \quad \text{Eq. 2-14}$$

$$\delta v = \frac{\boldsymbol{\lambda}}{2\boldsymbol{m} T_s} \quad \text{Eq. 2-15}$$

$$\delta v = \frac{\boldsymbol{\lambda f_s}}{4\boldsymbol{N}\boldsymbol{m}} \quad \text{Eq. 2-16}$$

$$I = \frac{\boldsymbol{f_s}}{2\boldsymbol{N}\boldsymbol{m}} \boldsymbol{T_i} \quad \text{Eq. 2-17}$$

$$B = \frac{\boldsymbol{c}}{2\boldsymbol{\delta r}} \quad \text{Eq. 2-18}$$

$$H = N \cdot \delta r \quad \text{Eq. 2-19}$$

2.3 Valid values and ranges of configurable parameters

Parameter	Unit	Valid values	Conditions
N		$2^4, 2^5, 2^6, 2^7, 2^8, 2^9$	$nM \leq 2^{13}$
$m\ (= M)$		$2^5, 2^6, 2^7, 2^8, 2^9$	
T_i	s	> 1	Steps of 1 s
δr	m	> 10	Steps of 1 m

2.4 Examples of some parameter configurations

For each choice of configurable variables specific values of dependent variables follow according to Eq. 2-1 - Eq. 2-19. The table below shows 5 choices of numbers of range gates, of spectral lines, and averaging time and the consequences for the most relevant dependent parameters, namely velocity range, velocity resolution, and number of incoherently averaged spectra.

In all cases $\boldsymbol{T_i}$ was set to 10 s. In examples (a) - (d) the highest possible product value $\boldsymbol{Nm} = 2^{13}$ was chosen. This choice leads to a velocity resolution of 0.19 m/s and to incoherent averaging over 305 measurements, regardless of the factors $\boldsymbol{N}$ and $\boldsymbol{m}$ (See Eq. 2-16 and Eq. 2-17)**.** The velocity range decreases with increasing number of range gates $\boldsymbol{N}$ from 48 to 6 m/s.

In case (e) a combination with $\boldsymbol{Nm} = 2^{12}$ was chosen. Here the velocity resolution is 0.38 m/s and the number of averaged spectra increases to 610. The velocity range (12 m/s) is the same as in example (c). The comparison of $\boldsymbol{N}$ and $\boldsymbol{m}$ in examples (c) and (e) illustrates that the velocity range is only a function of $\boldsymbol{N}$ – and not of the number of spectral lines $\boldsymbol{m}$, which may be a bit counter-intuitive. (See Eq. 2-6).

		Examples				
Parameter	**Unit**	**(a)**	**(b)**	**(c)**	**(d)**	**(e)**
$\boldsymbol{N}$		32	64	128	256	128
$\boldsymbol{m}$		256	128	64	32	32
$\boldsymbol{T_i}$	s	10	10	10	10	10
v_{ny}	m/s	48	24	12	6	12
δv	m/s	0.19	0.19	0.19	0.19	0.38
I		305	305	305	305	610

3 References

Atlas, D., R. Srivastava und R. Sekhon, 1973: Doppler radar characteristics of precipitation at vertical incidence, Rev. Geophys. Space Phys., 11:1-35.

Foote, G. B., and duToit, P.S., 1969: Terminal velocity of raindrops aloft, J. Appl. Meteorol., 8:249-253.

Gunn, R. und G. Kintzer, 1949: The terminal velocity of fall for water droplets in stagnant air, J. Meteor., 6:243-248.

Hildebrand, P.H. and R.S. Sekhon, 1974: Objective Determination of the Noise Level in Doppler Spectra, J. Appl.Meteor., 13, 808-811.

Klugmann, D. und C. Richter, 1995: Correction of Drop Shape-Induced Errors on Rain Rates Derived from Radar-measured Doppler Spectra at Vertical Incidence, J. Atmos. Ocean. Tech., 12, 657-661.

Mie, G., 1908: Beiträge zu Optik trüber Medien, speziell kolloidaler Metalllösungen, Ann. Phys. Folge 4, Bd. 25, 377-445.-

Peters, G., B. Fischer, H. Münster, M. Clemens, A. Wagner, 2005: Profiles of Raindrop Size Distributions as Retrieved by Microrain Radars. J. Appl. Meteor., 44, 1930-1949

Peters, G., B. Fischer, M. Clemens, 2010: Rain Attenuation of Radar Echoes Considering Finite-Range Resolution and Using Drop Size Distributions. J. Atmos. Oceanic Technol., 27, 829-842

Richter, C., 1993: Niederschlagsmessungen mit dem vertikal gerichteten FM-CW-Dopplerradar-RASS-System, Validierung und Anwendung, Dissertation Universität Hamburg, 143 pp.

Strauch, R.G., W.C. Campbell, R.B. Chadwick, K.P. Moran: FM-CW boundary layer radar with Doppler capability, NOAA Techn. Rep. ERL 329-WPL 39, Dept. of Commerce, May 1975.